

An Observer-Based Key Agreement Scheme for Remotely Controlled Mobile Robots

Amir Mohammad Naseri, Walter Lucia, Amr Youssef

Concordia Institute for Information Systems Engineering (CIISE)
Montreal, Quebec, Canada.

e-mail:{amirmohammad.naseri,walter.lucia,amr.youssef}@concordia.ca

Abstract: Remotely controlled mobile robots are important examples of Cyber-Physical Systems (CPSs). Recently, these robots are being deployed in many safety critical applications. Therefore, ensuring their cyber-security is of paramount importance. Different control schemes that have been proposed to secure such systems against sophisticated cyber-attacks require the exchange of secret messages between their smart actuators and the remote controller. Thus, these schemes require pre-shared secret keys, or an established Public Key Infrastructure (PKI) that allows for key agreement. Such cryptographic approaches might not always be suitable for the deployment environments of such remotely mobile robots. To address this problem, in this paper, we consider a control theoretic approach for establishing a secret key between the remotely controlled robot and the networked controller without resorting to traditional cryptographic techniques. Our key agreement scheme leverages a nonlinear unknown input observer and an error correction code mechanism to allow the robot to securely agree on a secret key with its remote controller. To validate the proposed scheme, we implement it using a Khepera-IV differential drive robot and evaluate its efficiency and the additional control cost acquired by it. Our experimental results confirm the effectiveness of the proposed key establishment scheme.

Keywords: Mobile robot security, differential-drive robot, key agreement, cyber-physical systems.

1. INTRODUCTION

Over the past recent years, the application of mobile robots in different safety critical domains, such as defence and space, search and rescue, health care, and industry 4.0, has gained an increasing interest (Tzafestas, 2013; Lewis and Ge, 2018; Fragapane et al., 2020). The research community has also been active in increasing the potential applications of these robots in networked and distributed control systems setup (Santilli et al., 2021; Klancar et al., 2017; Liu et al., 2018; Wang et al., 2021). On the other hand, such developments raise the concern of security and privacy of such systems (Dutta and Zielińska, 2021; Li et al., 2022; Wang et al., 2022). Mass adoption of robots leads to an increase in the possibilities of cyberattacks against these systems.

Different robotics cybersecurity issues, vulnerabilities threats, and risks have been classified and discussed in (Yaacoub et al., 2021). The target of an attacker can be any components of the Confidentiality, Integrity, Availability (CIA) triad on the level of the hardware of the robot, its firmware, or its communication channels (Yaacoub et al., 2021). Unlike cybersecurity of information technology systems, robots add the additional factor of physical interaction with the environment. While taking the control of a desk-top computer or a server may result in loss of information,

taking the control of a robot may directly result in physical damages and endangering whatever or whoever is nearby. In this paper, we focus on applications where mobile robots are remotely controlled, i.e., where the control inputs and sensor measurements are transmitted over insecure communication channels.

To guarantee any component of the CIA triad between the robot and the networked controller, or for the purpose of detection of different classes of cyberphysical attacks, in most of the proposed methods, sharing a secret key/seed is required. For example, the authors of (Noura et al., 2018) developed a physical-layer encryption algorithm for wireless machine-to-machine devices, in which sharing secret seeds is required for the implementation of the algorithm. On the other hand, the solution in (Noura et al., 2022) deals with the data integrity and source authentication problems, particularly for IoT devices. The proposed message authentication algorithm requires a secret seed/key to initialize the algorithm. Similarly, it is well-understood in the CPS community that to detect intelligent coordinated networked attacks such as covert attacks (Smith, 2015), proactive detection actions must be coordinately taken in both sides of the communication channels (Ghaderi et al., 2020). For example, moving-target (Griffioen et al., 2020) and sensor coding (Miao et al., 2016) based detection schemes implement such an idea to prevent the existence of undetectable attack, and both requires, for coordination purposes, that a secret seed is pre-shared between the plant and the controller. An anomaly detection scheme,

¹ This work is supported by the Natural Sciences and Engineering Research Council of Canada (NSERC).

specifically targeting differential-drive robots, is developed in (Cersullo et al., 2022), where intelligent setpoint attacks are of interest. The proposed detector leverages two command governor modules and two pseudo-random number generators (each placed in one of the two sides of the network). It has been proved that such an architecture prevent the existence of undetectable setpoint attacks only if a shared seed between the two sides of the communication channel can be established.

From the above examples, it is clear that the key-establishment problem in cyber-physical systems, including mobile robots, is relevant for enhancing the security of such systems.

1.1 Background and Related Works

Traditionally, key agreement is achieved through the use of symmetric or public key cryptographic protocols (Menezes et al., 2018). For example, using elliptic curve cryptography, in (Jain et al., 2021), the authors proposed a mutual authentication and key agreement scheme between cloud-based robots (i.e., robots that access cloud resources) and cloud servers. However, such solutions might not always be usable for robotic systems. Public key protocols are computationally demanding and require a public key infrastructure (Menezes et al., 2018) and the support of a key revocation mechanism (e.g., see (Shi et al., 2021)). These requirements make public key protocol impractical for robots with limited computational capabilities (Yaacoub et al., 2021). On the other hand, symmetric key-based solutions assume the existence of a pre-shared key. However, the compromise of such long-term keys usually leads to compromising the security of the whole system.

Alternative key-establishing solutions leverage the seminal concept of wiretap channel introduced by Wyner in (Wyner, 1975). Such schemes are not based on traditional cryptographic mechanisms. Instead, they utilize the role of noise, which is a natural characteristic in any communications system, to achieve secure communications. In particular, Wyner proved that if the communication channel between the sender and receiver is statistically better than the one from the sender to the eavesdropper, then it is possible to design an encoding mechanism to communicate with perfect secrecy. Over the years, such a concept has been leveraged to design different key-agreement protocols for CPSs, see, e.g., (Maurer, 1993; Ahlswede and Csiszár, 1993; Lara-Nino et al., 2021; Sutrala et al., 2021; Zhang et al., 2017; Rawat et al., 2017) and references therein. In (Maurer, 1993; Ahlswede and Csiszár, 1993), a key-agreement protocol based on public discussion is proposed. In (Sutrala et al., 2021), by considering a 5G-enabled industrial CPSs, a three-factor user authenticated key agreement protocol is developed; in (Zhang et al., 2017), by using ambient wireless signals, a cross-layer key establishment model for wireless devices in CPSs is designed to allow devices to extract master keys at the physical layer. In (Rawat et al., 2017), by exploiting an information-theoretic approach, the outage probability for secrecy rate in multipleinput multiple-output (MIMO) systems for CPSs is investigated.

While all the above solutions are developed for CPSs, none of them takes advantage of the closed-loop dynamics of

the underlying physical system dynamics to design the key agreement protocol. A first tentative to design a key agreement leveraging the physical properties of control systems can be found in (Li et al., 2011), where the authors exploited common information about the plant’s state to establish a key between the sensor and the controller. However, the authors only consider the case where the eavesdropper cannot observe the plant’s state. More recently, in (Lucia and Youssef, 2020, 2022), control theoretical approaches have been proposed to design key-agreement scheme leveraging the asymmetry in the CPS model knowledge available to the defender and adversary.

1.2 Contribution

Existing control-theoretical solutions targeting generic CPSs (Lucia and Youssef, 2020, 2022) are developed under the assumptions of linear plant’s dynamics (which is not the case for mobile robots) and they have never tested on a real testbed. Consequently, in a nutshell, this work presents the following theoretical and practical contributions:

- It extends the key-establishment solution in (Lucia and Youssef, 2022) to deal with the non-linear dynamics of mobile robots.
- It experimentally validates, using a remotely maneuvered Khepera IV² mobile robot, the performance and the capacity of the proposed control theoretical key-agreement scheme.

1.3 Notation and Paper Organization

The set of real numbers and real-valued column vectors of dimension $n_r > 0$ are denoted with \mathbb{R} and \mathbb{R}^{n_r} , respectively. $M \in \mathbb{R}^{n_r \times n_c}$ denotes a real-valued matrix of size $n_r \times n_c$. Moreover, $I_{n_1} \in \mathbb{R}^{n_1 \times n_1}$, $0_{n_0} \in \mathbb{R}^{n_0 \times n_0}$, and $1_{n_1} \in \mathbb{R}^{n_1}$ denote the identity matrix, zero matrix, and all-ones column vector, respectively. The sets of non-negative integer numbers and positive integer number is denoted by \mathbb{Z}_+ and $\mathbb{Z}_{>0}$. The transpose and inverse of matrix M are denoted with M^T and M^{-1} , respectively. Given a random variable $v \in \mathbb{R}^{n_r}$, $v \sim \mathcal{N}(\mu_{n_r}, \Sigma_{n_r})$ indicates a random variable normally distributed with mean $\mu_{n_r} \in \mathbb{R}^{m_r}$ and covariance matrix $\Sigma_{n_r} > 0 \in \mathbb{R}^{n_r \times n_r}$. Given an event E , the probability of occurrence of such event is denoted with $P(E)$. Given a binary string $s \in \{0, 1\}^{n_s}$, $s[i]$ denotes the i -th bit of s .

The rest of the paper is organized as follows. In Section 2, first, the robot model and the adversary are presented, then, the considered key-establishment problem is stated. In Section 3, the proposed protocol for the key agreement is described. Experimental results obtained using a Khepera IV differential-drive robot are presented in Section 4. Finally, Section 5 concludes the paper with some final remarks.

2. PRELIMINARIES AND PROBLEM FORMULATION

Definition 1. Given three positive integers $n_c \in \mathbb{Z}_{>0}$, $k_c \in \mathbb{Z}_{>0}$, $d_c \in \mathbb{Z}_{>0}$, a linear Error Correcting Code (ECC) de-

² <http://www.k-team.com/khepera-iv>

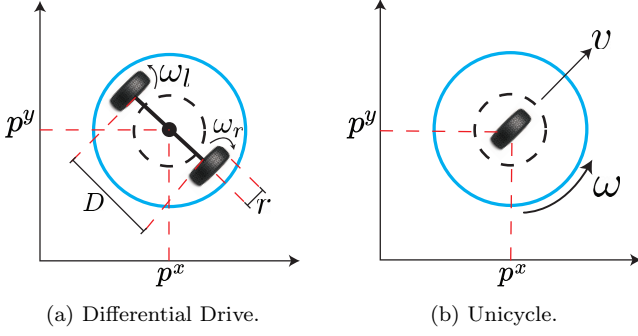


Fig. 1. Differential-drive and unicycle models.

finds a linear transformation of a binary string $s \in \{0, 1\}^{k_c}$ into a subspace $\mathcal{C} \in \{0, 1\}^{n_c}$ of cardinality 2^{k_c} such that

- $\forall (c_1, c_2) \in \mathcal{C}, c_1 \neq c_2$, the Hamming distance $d_H(c_1, c_2) < d_c$.
- the maximum number of errors that can be corrected is $\frac{d_c - 1}{2}$.

□

In what follows, we consider a scenario where a mobile robot is manoeuvred by a networked controller and the network infrastructure is vulnerable to eavesdropping attacks.

2.1 Robot Model

Among different existing categories of mobile robots, wheeled-mobile robots are very common for ground vehicles and they find application in different domains such as surveillance and warehouse automation. Moreover, among the nonholonomic configurations, the differential-drive structure, characterized by two rear independently-driven wheels and one or more front castor wheels for body support, is often adopted in the industry (Martins et al., 2017). A schematic of a differential-drive robot is shown in Fig. 1a.

The pose of a differential-drive robot is described by the planar coordinates (p^x, p^y) of its center of mass and orientation θ (see Fig. 1a). By resorting to the forward Euler discretization method and a sampling time $T > 0$, the discrete-time kinematic model of the differential-drive is given by (De Luca et al., 2001):

$$\begin{aligned} p^x(k+1) &= p^x(k) + \frac{Tr}{2} \cos \theta(k) (\omega_r(k) + \omega_l(k)) + \zeta^{p^x}(k) \\ p^y(k+1) &= p^y(k) + \frac{Tr}{2} \sin \theta(k) (\omega_r(k) + \omega_l(k)) + \zeta^{p^y}(k) \\ \theta(k+1) &= \theta(k) + \frac{Tr}{D} (\omega_r(k) - \omega_l(k)) + \zeta^\theta(k) \end{aligned} \quad (1)$$

where $r > 0$ is the radius of the wheels, $D > 0$ the rear axle length, and $u^D = [\omega_r, \omega_l]^T \in \mathbb{R}^2$ the control input vector, which consists of the angular velocities of the right and left wheel, respectively. $\zeta(k) = [\zeta^{p^x}(k), \zeta^{p^y}(k), \zeta^\theta(k)]^T \sim \mathcal{N}(0, \mathcal{W})$ is the process noise with $\mathcal{W} \in \mathbb{R}^{3 \times 3}$. Let $x(k) = [p^x(k), p^y(k), \theta(k)]^T \in \mathbb{R}^3$ denote the robot's state vector. It is assumed that $x(k)$ can be estimated leveraging the measurement vector $y(k) \in \mathbb{R}^{n_p}$, $n_p > 0$, obtained via odometric calculations and/or exteroceptive (e.g., sonar, laser) sensors (D'Alfonso et al., 2015), i.e.,:

$$y(k) = h(x(k)) + \xi(k) \quad (2)$$

where $h(x(k))$ denotes the nonlinear output equation, and $\xi(k) \sim (0, \mathcal{V})$, $\mathcal{V} \in \mathbb{R}^{n_p \times n_p}$, the measurement noise, uncorrelated with $\zeta(k)$.

By denoting with $v(k)$ and $\omega(k)$ the linear and angular velocities of the center of mass of the robot, it is possible to apply to (1) the transformation

$$\begin{bmatrix} v(k) \\ \omega(k) \end{bmatrix} = H \begin{bmatrix} \omega_r(k) \\ \omega_l(k) \end{bmatrix}, \quad H := \begin{bmatrix} \frac{r}{2} & \frac{r}{2} \\ r & -r \\ \frac{D}{D} & \frac{D}{D} \end{bmatrix} \quad (3)$$

and describe the robot behaviour by means of the following unicycle model (see Fig. 1b):

$$\begin{aligned} p^x(k+1) &= p^x(k) + Tv(k) \cos \theta(k) + \zeta^{p^x}(k) \\ p^y(k+1) &= p^y(k) + Tv(k) \sin \theta(k) + \zeta^{p^y}(k) \\ \theta(k+1) &= \theta(k) + T\omega(k) + \zeta^\theta(k) \end{aligned} \quad (4)$$

where $u^U(k) = [v(k), \omega(k)]^T \in \mathbb{R}^2$ is the control input vector of the unicycle.

2.2 Adversary Model

We assume a passive adversary capable of eavesdropping the control input and sensor measurements transmitted between the plant and the networked controller, see Eve in Fig. 2. We also assume that the adversary is aware that the robot is a differential-drive robot but it might not have exact knowledge of all the robot's parameters (e.g., T, r, D, \mathcal{W}) and robot's measurement function (e.g., $h(\cdot)$ and \mathcal{V}). Therefore, we assume that the adversary has the following model:

$$\begin{aligned} p_a^x(k+1) &= p^x(k) + \frac{T_a r_a}{2} \cos \theta_a(k) (\omega_r(k) + \omega_l(k)) + \zeta_a^{p^x}(k) \\ p_a^y(k+1) &= p^y(k) + \frac{T_a r_a}{2} \sin \theta_a(k) (\omega_r(k) + \omega_l(k)) + \zeta_a^{p^y}(k) \\ \theta_a(k+1) &= \theta(k) + \frac{T_a r_a}{D_a} (\omega_r(k) - \omega_l(k)) + \zeta_a^\theta(k) \\ y_a(k) &= h_a(x_a(k)) + \xi_a(k) \end{aligned} \quad (5)$$

where $\zeta_a = [\zeta_a^{p^x}(k), \zeta_a^{p^y}(k), \zeta_a^\theta(k)]^T \sim (0, \mathcal{W}_a)$, $\xi_a^x(k) \sim (0, \mathcal{V}_a)$, and $(T_a, r_a, d_a, h_a(\cdot), \mathcal{W}_a, \mathcal{V}_a)$ are the adversary estimations for the robot's model (1)-(2).

Assumption 1. Let $\mathcal{M} = \{T, r, D, \mathcal{W}, h(\cdot), \mathcal{V}\}$ and $\mathcal{M}_a = \{T_a, r_a, D_a, \mathcal{W}_a, h_a(\cdot), \mathcal{V}_a\}$ be the robot's model knowledge available to the controller's designer and to the adversary, respectively. Then,

$$\mathcal{M} \neq \mathcal{M}_a \quad (6)$$

Remark 1. The model discrepancy (6) might arise for different reasons. First, the adversary might not be aware of the robot construction parameters r, D or the output function $h(\cdot)$. Instead, the attacker might just be able to estimate them using identification techniques or by inspection (e.g., via cameras). Second, while the defender can estimate \mathcal{W}, \mathcal{V} by performing offline experiments, see, e.g., (Antonelli and Chiaverini, 2007; D'Alfonso et al., 2015), the eavesdropper can only perform online identification procedure relying on the online robot operations, which might be unsuitable for system identification purposes.

2.3 Problem Formulation

The here considered key-agreement problem can be stated as follows.

Problem 1. Consider the robot and adversary models (1)-(6). Without resorting to traditional cryptographic schemes, design a key agreement protocol between the robot and the networked controller such that the keys of length $n > 0$ identified by the controller ($\mathcal{K}_c \in \{0, 1\}^n$), robot ($\mathcal{K}_r \in \{0, 1\}^n$) and attacker ($\mathcal{K}_a \in \{0, 1\}^n$) are such that

$$P\{\mathcal{K}_c = \mathcal{K}_r\} \approx 1 \text{ and } P\{\mathcal{K}_c \neq \mathcal{K}_a\} \approx 1 \quad (7)$$

3. KEY AGREEMENT PROTOCOL

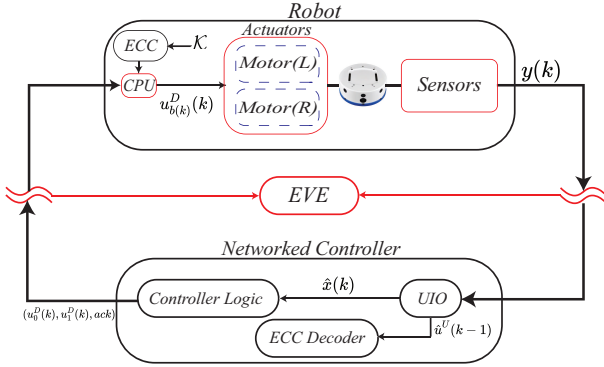


Fig. 2. Control architecture for the proposed key agreement protocol.

As proved in (Lucia and Youssef, 2020), the asymmetry (6) in the plant model knowledge is sufficient to ensure the existence of a Wyner wiretap-like channel in networked cyber-physical systems. The latter is here leveraged to design an encoding mechanism for the considered key-exchange problem. In particular, the proposed key-agreement protocol is developed under the following assumptions.

Assumption 2. The available sensor measurements are sufficiently rich to allow the existence of an Unknown Input Observer (UIO) capable of simultaneously estimate $x(k)$ and $u^D(k)$ from the available measurement vector $y(k)$. By denoting with $\hat{x}(k)$ and $\hat{u}^D(k)$ the estimated vectors, the UIO is abstractly modeled as the following recursive function

$$[\hat{u}^D(k-1), \hat{x}(k)] = UIO(u^D(k), \hat{x}(k-1), y(k), \mathcal{M}) \quad (8)$$

where $(\hat{u}^D(k-1), \hat{x}(k))$ and $(\hat{u}^D(k-2), \hat{x}(k-1))$ are the available estimations at time steps k and $k-1$, respectively. Moreover, the eavesdropper is able to run the same UIO as in (8) with \mathcal{M}_a instead of \mathcal{M} .

In the sequel, we assume that the robot is equipped with a tracking controller which provides the control vector $u^U(k), \forall k$, i.e.,

$$u^U(k) = \begin{bmatrix} v(k) \\ \omega(k) \end{bmatrix} = f_c(x(k), x_r(k), \dot{x}_r(k), \ddot{x}_r(k)) \quad (9)$$

where $f_c(\cdot, \cdot, \cdot)$ denotes a generic controller, $x_r(k) \in \mathbb{R}^3, \dot{x}_r(k) \in \mathbb{R}^3, \ddot{x}_r(k) \in \mathbb{R}^3$ are the reference state, velocity and acceleration vectors, respectively (De Luca et al., 2001).

By referring to the networked control system architecture illustrated in Fig. 2, the idea behind the proposed key-agreement protocol can be described in four points:

(P1) - The controller computes $u^U(k)$ as in (9). Then, it generates two perturbed control inputs, namely $u_0^U(k) \in \mathbb{R}^2$ and $u_1^U(k) \in \mathbb{R}^2$, by adding and subtracting a small bias vector $\Delta \in \mathbb{R}^2$ to $u^U(k)$, i.e.,

$$u_0^U(k) = u^U(k) + \Delta, \quad u_1^U(k) = u^U(k) - \Delta \quad (10)$$

where $\Delta = [\Delta_v, \Delta_\omega]^T$, $\Delta_v \geq 0, \Delta_\omega \geq 0$ and such that $\Delta_v + \Delta_\omega > 0$ (i.e., at least one between Δ_v and Δ_ω must be strictly greater than zero). Finally, the differential-drive control inputs are computed as $u_0^D(k) = H^{-1}u_0^U(k)$ and $u_1^D(k) = H^{-1}u_1^U(k)$, see (10), and the pair $(u_0^D(k), u_1^D(k))$ is sent to the robot.

(P2) - Once the robot receives $(u_0^D(k), u_1^D(k))$, its CPU unit is in charge of deciding which one of the two control inputs should be used. To this end, it generates a random bit $b(k) \in \{0, 1\}$ and send to the actuators $u_{b(k)}^D(k)$. Note that the bit $b(k)$ and, consequently, the control signal applied to the robot $(u_{b(k)}^D(k))$ are unknown to the networked controller and to the eavesdropper. At each iteration, the robot appends $b(k)$ to the local key \mathcal{K}_r .

(P3) - When the networked controller receives $y(k)$, it can run the UIO (8) and obtain the estimated pair $(\hat{x}(k), \hat{u}^D(k-1))$. Moreover, since also the pair $(u_0^D(k-1), u_1^D(k-1))$ is known, the controller can estimate the random bit $b(k-1)$ (used by the robot) as

$$\hat{b}(k-1) = \begin{cases} 0 & \text{if } d_0 < d_1 \\ 1 & \text{if } d_1 < d_0 \end{cases} \quad (11)$$

where d_0 and d_1 are the distances between the estimated control input $\hat{u}^D(k-1)$ and $(u_0^D(k-1), u_1^D(k-1))$, i.e.,

$$\begin{aligned} d_0(k-1) &= \|\hat{u}^D(k-1) - u_0^D(k-1)\|_2, \\ d_1(k-1) &= \|\hat{u}^D(k-1) - u_1^D(k-1)\|_2 \end{aligned} \quad (12)$$

At each iteration, the networked controller appends $\hat{b}(k)$ to the local key \mathcal{K}_c .

(P4) - The adversary can run the UIO (8) with \mathcal{M}_a instead of \mathcal{M} and obtain a local estimation, namely $\hat{b}_a(k-1)$, of $b(k-1)$, to append to its local key \mathcal{K}_a . However, given the model discrepancy (6), the covariance of the unknown input estimation error for the attacker is expected to be larger of the one obtained by the networked controller (Lucia and Youssef, 2022). Consequently, for a proper choice of Δ , it is expected that $P\{\mathcal{K}_c = \mathcal{K}_r\} \approx 1$ and $P\{\mathcal{K}_c \neq \mathcal{K}_a\} \approx 1$.

Note that the above described UIO-based decoding scheme might not be robust against possible model mismatches and/or process and measurement noises. To make the protocol more robust, we enhance its decoding operations by means of an Error Correcting Code (ECC) scheme and a feedback acknowledgment signal, namely *ack*, which is sent by the controller along with the pair of control inputs.

By assuming, for the sake of simplicity and clarity, a linear ECC, the ECC and *ack* feedback signal are used as follows (refer to Definition 1 for the used notation and terminology):

- The robot splits a randomly generated local key \mathcal{K} into a sequence of substring s_i . Each s_i is encoded into a sequence of codewords c_i . Each bit of c_i , namely $c_i[j]$, is sequentially used to decide $b(k)$ in (P2), i.e., $b(k) = c_i[j]$.
- The robot estimates $\hat{b}(k)$ as in (P3) and collects them to obtain an estimation of the codewords c_i , namely \hat{c}_i . Then, the Hamming distance $d_{\hat{c}_i}$ is evaluated

$$d_{\hat{c}_i} = \arg \min_{c \in \mathcal{C}} d_H(c, c_i) \quad (13)$$

If $d_{\hat{c}_i}$ is much smaller than the number of correctable errors, then the codeword is accepted, the binary string \hat{s}_i (associated to \hat{c}_i via ECC) is appended \mathcal{K}_c , and a positive $ack_i = 1$ is sent. Otherwise, the codeword is discarded and $ack_i = 0$ is sent.

- The robot, for every received $ack_i = 1$, append c_i to \mathcal{K}_r .

The complete key-agreement protocol is summarized in Algorithm 1.

Algorithm 1: Proposed Key Agreement Protocol

```

/*Robot                                     */
1 Initialization: Generate  $\mathcal{K}$ , and set  $\mathcal{K}_r = \emptyset$ . Split  $\mathcal{K}$ 
  into sub-strings  $s_i \in \{0, 1\}^{k_c}$ 
2 Sequentially encode each  $s_i$  into codewords
   $c_i \in \{0, 1\}^{n_c} \in \mathcal{C}$ 
3 At each time step  $k$ :
  - Sequentially use each bit  $c_i[j]$  of  $c_i$  to pick
     $b(k) = c_i[j]$  and apply to the robot  $u_{b(k)}^D(k)$ 
  - When all  $n_c$  bits of  $s_i$  are used, the robot
    receives  $ack \in \{0, 1\}$  from the controller
  if  $ack == 1$  then
    |  $s_i$  is appended to  $\mathcal{K}_r$ 
  else
    |  $s_i$  is discarded
  end

/*Controller                                 */
1 Initialization: Set  $\mathcal{K}_c = \emptyset$ .
2 At each time step  $k$  :
  - the pair  $(\hat{u}^D(k-1), \hat{x}(k))$  and  $\hat{b}(k-1)$  are
    estimated using (8) and (11), respectively.
  -  $\hat{b}(k-1)$  is appended to the estimated codeword
     $\hat{c}_i$ 
  - When  $n_c$  bits of  $\hat{c}_i$  are estimated, the distance
     $d_{\hat{c}_i}$  is computed using (13).
  if  $d_{\hat{c}_i} \ll \frac{d_c-1}{2}$  then
    | The codeword  $\hat{c}_i$  is considered valid
    |  $\hat{s}_i$  is decoded from  $\hat{c}_i$  and appended to  $\mathcal{K}_c$ ;
    | send  $ack = 1$ 
  else
    | The codeword  $\hat{c}_i$  is considered invalid and
    | discarded; send  $ack = 0$ 
  end
  - Compute  $(u_0^D(k), u_1^D(k))$  as in (10) and send it

```

Remark 2. The bias Δ in (10) and the ECC parameters (n_c, k_c, d_c) are design parameters that can be tuned to achieve $P\{\mathcal{K}_c = \mathcal{K}_r\} \approx 1$. Moreover, to ensure the correctness of the exchanged key, the controller and the robot can

always publicly verify its correctness exchanging the hash values associated to \mathcal{K}_c and \mathcal{K}_r . Moreover, to eliminate the partial key knowledge gained by the adversary, the controller and the robot can also enhance the security of the exchanged key by means of standard privacy amplification procedures, see, e.g., (Van Assche, 2006; Bennett et al., 1995).

4. EXPERIMENTAL RESULTS

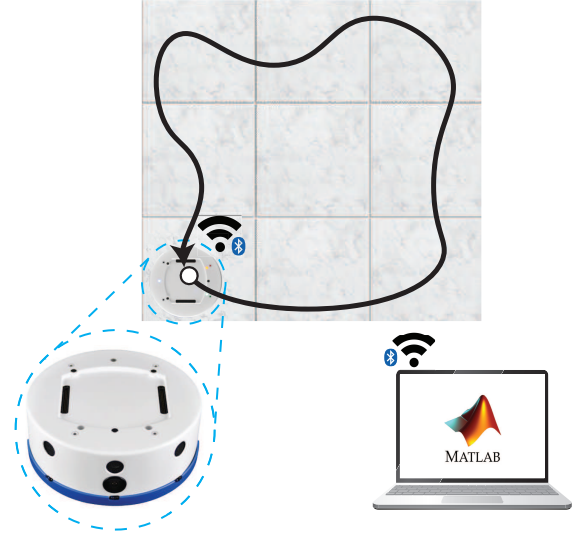


Fig. 3. Experimental setup.

In this section, the effectiveness of the proposed key-agreement protocol is verified by means of the experimental setup shown in Fig. 3. The setup consists of:

- A laptop where a tracking controller is implemented in Matlab.
- A Khepera IV differential-drive robot.
- A Bluetooth 4.0 communication channel between the robot and the laptop for the two-way exchange of data, i.e., control inputs and sensor measurements.

4.1 Khepera IV robot

The Khepera-IV robot, produced by K-Team, is a differential drive robot whose discrete-time kinematic model is as in (1), where, $r = 0.021 [m]$ and $D = 0.1047 [m]$, $\mathcal{W} = 10^{-2}I_3$, and the maximum angular velocities of the wheels is of $38 [rad/sec]$. On the other hand, the used measurement vector $y(k)$ consists of the wheels encoder measurements that, via odometric calculations, allow to obtain an estimation of the entire state of the robot (De Luca et al., 2001). Consequently, the output equation (2) is modeled as $y(k) = x(k) + \xi(k)$ with $\xi(k)$ a Gaussian noise with covariance matrix $\mathcal{V} = 10^{-4}I_3$.

In the performed experiments, the robot's processing unit is equipped with a server that receives and sends, via Bluetooth, the control inputs and sensor measurements. The used sampling time is $T_s = 0.2 [sec]$.

4.2 UIO, tracking Controller, and reference trajectory

UIO: The unicycle model (4) under the control law (10) can be re-written (for compactness) as

$$x(k+1) = f(x(k), u^U(k) + \Delta_u) + \zeta(k), \quad (14)$$

with Δ_u the unknown bias of value $\pm\Delta$. Then, the extended Kalman filter with unknown input estimation algorithm proposed in (Guo, 2018, Appendix A) has been used to implement the UIO module (8). For completeness, the UIO operations, adapted to the considered setup, are reported in Algorithm 2, where, $P_0^x = 0_{3 \times 3}$, $\hat{x}_0 = [0, 0, 0]^T$, and A_k, B_k, G_k are the matrices characterizing the linearization $x(k+1) = A_k x(k) + B_k u^U(k) + G_k \Delta_u(k)$ of (14) along the state and input trajectories, i.e.,

$$A_k \triangleq \left. \frac{\partial f}{\partial x} \right|_{(\hat{x}_{k|k}, u^U(k))}, \quad B_k \triangleq \left. \frac{\partial f}{\partial u} \right|_{(\hat{x}_{k|k}, u^U(k))}, \quad (15)$$

$$G_k \triangleq \left. \frac{\partial f}{\partial \Delta_u} \right|_{(\hat{x}_{k|k}, u^D(k))}$$

Consequently, $\hat{u}^D(k-1) = H^{-1}(u^U(k) + \hat{\Delta}_u(k-1))$.

Algorithm 2: Non-Linear Unknown Input Observer

```

Input:  $u(k-1), \hat{x}_{k-1}, y(k)$ 
Output:  $\hat{x}_k, \Delta_u(k-1)$ 

/*Input Estimation */
1  $\tilde{P}_{k-1} = A_{k-1} P_{k-1}^x (A_{k-1})^T + W$ 
2  $\tilde{R}_k^* = \tilde{P}_{k-1} + \mathcal{V}$ 
3  $\Xi_k = (G_{k-1})^T (\tilde{R}_k^*)^{-1}$ 
4  $M_k = (\Xi_k G_{k-1})^{-1} \Xi_k$ 
5  $\hat{\Delta}_u(k-1) = M_k (y(k) - f(\hat{x}_{k-1}, u(k-1)))$ 
6  $P_{k-1}^a = M_k \tilde{R}_k^* (M_k)^T$ 

/*State Prediction */
7  $\hat{x}_{k|k-1} = f(\hat{x}_{k-1}, u(k-1) + \hat{\Delta}_u(k-1))$ 
8  $\Phi_k = (I - G_{k-1} M_k)$ 
9  $\bar{A}_{k-1} = \Phi_k A_{k-1}$ 
10  $\bar{Q}_{k-1} = \Phi_k Q_{k-1} (\Phi_k)^T + G_{k-1} M_k R_k (M_k)^T (G_{k-1})^T$ 
11  $P_{k|k-1}^x = \bar{A}_{k-1} P_{k-1}^a (\bar{A}_{k-1})^T + \bar{Q}_{k-1}$ 

/*State Estimation */
12  $\Gamma_k = G_{k-1} M_k$ 
13  $\tilde{R}_k = P_{k|k-1}^x + R_k + \Gamma_k R_k + R_k (\Gamma_k)^T$ 
14  $L_k = P_{k|k-1}^x + R_k (M_k)^T (G_{k-1})^T \tilde{R}_k^{-1}$ 
15  $\hat{x}_k = \hat{x}_{k|k-1} + L_k (y(k) - h_2(\hat{x}_{k|k-1}))$ 
16  $\Psi_k = I - L_k$ 
17  $P_k^x = \Psi_k P_{k|k-1}^x \Psi_k^T + L_k R_k (L_k)^T - \Psi_k G_{k-1} M_k R_k (L_k)^T - L_k R_k (M_k)^T (G_{k-1})^T (\Psi_k)^T$ 

```

Tracking controller: The robot's is controlled using the nonlinear controller based on dynamic feedback linearization described in (De Luca et al., 2001, Eq. 5.18). By denoting the reference trajectory and its first and second derivatives along the p^x and p^y axis as (p_r^x, p_r^y) , $(\dot{p}_r^x, \dot{p}_r^y)$, $(\ddot{p}_r^x, \ddot{p}_r^y)$, the control law is

$$\begin{aligned} v(k) &= \ddot{p}_r^x(k) + k_p^x (p_r^x(k) - p^x(k)) + k_d^x (\dot{p}_r^x(k) - \dot{p}^x(k)) \\ \omega(k) &= \ddot{p}_r^y(k) + k_p^y (p_r^y(k) - p^y(k)) + k_d^y (\dot{p}_r^y(k) - \dot{p}^y(k)) \end{aligned} \quad (16)$$

In the performed experiments, the controller has been implemented in Matlab using $k_p^x = k_p^y = 1.10$, and $k_d^x = k_d^y = 0.80$.

Reference Trajectory: The reference signal is the square-shaped trajectory shown in Fig. 6. The square's vertices are $\{(0, 0), (1, 0), (1, 1), (0, 1)\}$ and the timing laws for (p_r^x, p_r^y) , $(\dot{p}_r^x, \dot{p}_r^y)$, $(\ddot{p}_r^x, \ddot{p}_r^y)$ have been obtained using the built-in Matlab function *cubicpolytraj* which has been configured to travel each side of the square in 17 [sec]. In the performed experiments, the square trajectory repeats three consecutive times.

4.3 Perturbed control inputs and ECC configuration

Perturbed control inputs: The pair $(u_0^U(k), u_0^D(k))$ has been obtained adding a small perturbation only into the linear velocity command $v(k)$ computed as in (16), i.e., $\Delta_v > 0$ and $\Delta_\omega = 0$, see (10).

ECC configuration: A simple repetition code has been used to implement the ECC. Therefore, the string s_i consists of a single bit of \mathcal{K} (i.e., $k_c = 1$) and the codewords c_i are vectors repeating s_i for n_c times. In the performed experiments, we set $n_c = 3$ and a codeword is accepted only if the number of decoding errors $d_{c_i} = 0$.

4.4 Results

The proposed key-agreement protocol (Algorithm 1) has been evaluated for 10 equally spaced value of $\Delta_v \in [0.02, 0.045]$. For each Δ_v , the experiment has been repeated 10 times and with different randomly generated keys \mathcal{K} of length 345 bits. The obtained results are shown in Figs. 4-7 where the shown boxplots describe the median, minimum and maximum values of each point.

Fig. 4 shows the percentages of accepted codewords and correctly decoded/agreed bits. The number of accepted codewords (red boxplot) increases with Δ_v , which implies that the capacity of the key agreement protocol improves with the magnitude of the state shift Δ_v . Moreover, for $\Delta_v \geq 0.035$ all the accepted bits (blue boxplot) are also correct. The latter is justified by the fact that by increasing Δ_v , the distance between u_0^D and u_1^D increases until a point where estimation errors provoked by the process and measurement noises becomes negligible.

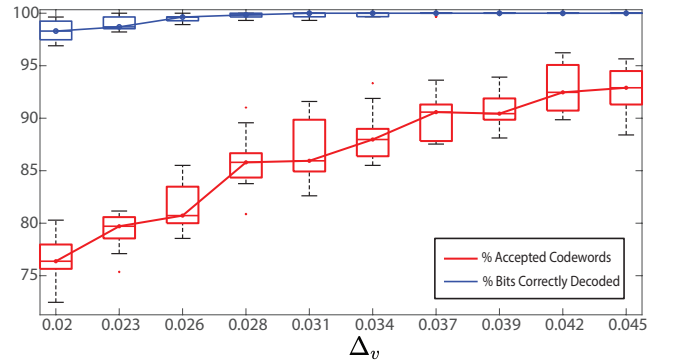


Fig. 4. Percentage of accepted codewords (red boxplot) and correctly decoded bits (blue boxplot) by the controller for $\Delta_v \in [0.02, 0.045]$.

On the other hand, Fig. 5 shows the average tracking error

$$J_x = \frac{1}{N_s} \sum_{k=1}^{N_s} \|[p^x(k), p^y(k)]^T - [p_r^x(k), p_r^y(k)]^T\|_2$$

of the robot for different values of Δ_v , where N_s is the number of discrete-time steps. As expected, also the tracking error of the robot increase with Δ_v . Consequently, the latter suggests that the smallest value of Δ_v ensuring zero decoding errors (i.e., $\Delta_v = 0.035$) should be used for key-agreement. The square-shaped reference trajectory (one lap) and the robot trajectories (one lap, single experiment) in the presence (for $\Delta_v = 0.035$) and in the absence (for $\Delta_v = 0$) of the proposed key-agreement protocol are shown in Fig. 6. There, it is possible to appreciate how the proposed key-agreement does not have a significant impact on robot reference tracking capabilities. A demo pertaining to Fig. 6 is available at the following weblink <https://youtu.be/9FJkQhJ8sdY>.

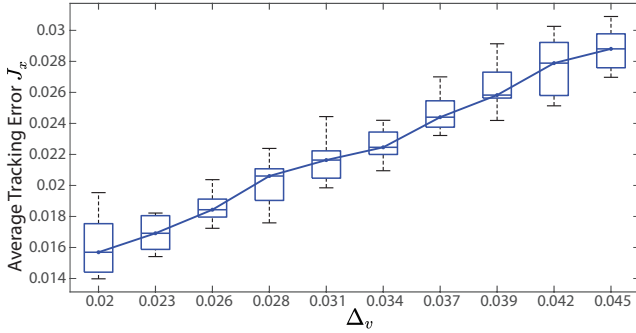


Fig. 5. Performance index J_x for $\Delta_v \in [0.02, 0.045]$.

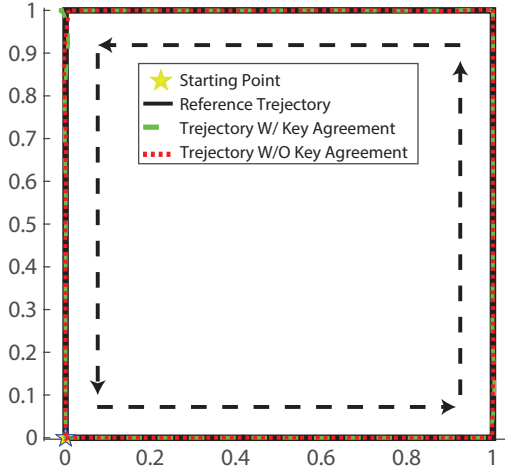


Fig. 6. Square-shaped reference trajectory and robot's trajectory with (for $\Delta_v = 0.035$) and without the proposed key-agreement protocol.

Finally, to test the capability of the adversary to intercept and decode the transmitted key, we have emulated an eavesdropper which has a non-perfect model knowledge \mathcal{M}_a . In particular, we have assumed that the attacker knows $r, d, \mathcal{W}, \mathcal{V}$ with a percentage error not superior to α . Moreover, for $\Delta_v = 0.035$, 10 equally spaced values of $\alpha \in \pm[0, 10]\%$ have been considered, and for each value of α , 10 experiments have been conducted with α randomly selected in the interval $[-\alpha, \alpha]$. Fig. 7 reports the results of such an experiment where the y-axis shows the % bit difference between the keys estimated by the controller (\mathcal{K}_c) and the adversary \mathcal{K}_a . As expected, the adversary conceptual channel becomes worse as the model uncertainty, i.e. α , increases.

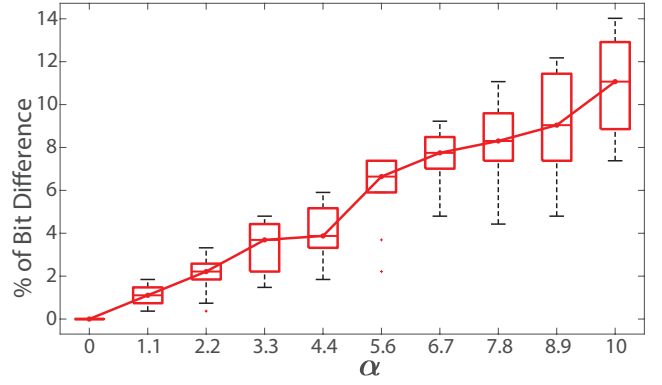


Fig. 7. Bits difference (% disagreement) between \mathcal{K}_c and \mathcal{K}_a for $\Delta_v = 0.035$ and $\alpha \in \pm[0, 10]\%$.

5. CONCLUSION

In this paper, we have developed a key-agreement protocol for remotely controlled mobile robots without resorting to traditional cryptographic approaches. In particular, we have leveraged the asymmetries between the controller's and adversary knowledge about the robot model to develop a key-exchange protocol based on a non-linear unknown input observer and an error correcting code mechanism. The proposed solution has been experimentally validated using a Khepera IV differential-drive robot, and the obtained results confirmed the effectiveness of the proposed design. Future studies will be devoted develop alternative protocol capable of increasing the throughput of the key-exchange mechanism.

REFERENCES

- Ahlsvede, R. and Csiszár, I. (1993). Common randomness in information theory and cryptography. i. secret sharing. *IEEE Transactions on Information Theory*, 39(4), 1121–1132.
- Antonelli, G. and Chiaverini, S. (2007). Linear estimation of the physical odometric parameters for differential-drive mobile robots. *Autonomous Robots*, 23(1), 59–68.
- Bennett, C.H., Brassard, G., Crépeau, C., and Maurer, U.M. (1995). Generalized privacy amplification. *IEEE Transactions on Information theory*, 41(6), 1915–1923.
- Cersullo, M., Tiriolo, C., Franzè, G., and Lucia, W. (2022). A detection strategy for setpoint attacks against differential-drive robots. In *IEEE International Conference on Automation Science and Engineering (CASE)*, 1035–1040.
- De Luca, A., Oriolo, G., and Vendittelli, M. (2001). Control of wheeled mobile robots: An experimental overview. *Ramsete*, 181–226.
- Dutta, V. and Zielińska, T. (2021). Cybersecurity of robotic systems: Leading challenges and robotic system design methodology. *Electronics*, 10(22), 2850.
- D'Alfonso, L., Lucia, W., Muraca, P., and Pugliese, P. (2015). Mobile robot localization via ekf and ukf: A comparison based on real data. *Robotics and Autonomous Systems*, 74, 122–127.
- Fragapane, G., Ivanov, D., Peron, M., Sgarbossa, F., and Strandhagen, J.O. (2020). Increasing flexibility and productivity in industry 4.0 production networks with autonomous mobile robots and smart intralogistics. *Annals of operations research*, 1–19.

- Ghaderi, M., Gheitasi, K., and Lucia, W. (2020). A blended active detection strategy for false data injection attacks in cyber-physical systems. *IEEE Transactions on Control of Network Systems*, 8(1), 168–176.
- Griffioen, P., Weerakkody, S., and Sinopoli, B. (2020). A moving target defense for securing cyber-physical systems. *IEEE Transactions on Automatic Control*, 66(5), 2016–2031.
- Guo, P. (2018). *Detection and Prevention: Toward Secure Mobile Robotic Systems*. The Pennsylvania State University.
- Jain, S., Nandhini, C., and Doriya, R. (2021). Ecc-based authentication scheme for cloud-based robots. *Wireless Personal Communications*, 117(2), 1557–1576.
- Klancar, G., Zdesar, A., Blazic, S., and Skrjanc, I. (2017). *Wheeled mobile robotics: from fundamentals towards autonomous systems*. Butterworth-Heinemann.
- Lara-Nino, C.A., Diaz-Perez, A., and Morales-Sandoval, M. (2021). Key-establishment protocols for constrained cyber-physical systems. In *Security in Cyber-Physical Systems*, 39–65. Springer.
- Lewis, F.L. and Ge, S.S. (2018). *Autonomous mobile robots: sensing, control, decision making and applications*. CRC Press.
- Li, H., Lai, L., Djouadi, S., and Ma, X. (2011). Key establishment via common state information in networked control systems. In *American Control Conference*, 2234–2239.
- Li, Y., He, J., Chen, C., and Guan, X. (2022). Intelligent physical attack against mobile robots with obstacle-avoidance. *IEEE Transactions on Robotics*. doi:10.1109/TRO.2022.3201394.
- Liu, A., Zhang, W.A., Yu, L., Yan, H., and Zhang, R. (2018). Formation control of multiple mobile robots incorporating an extended state observer and distributed model predictive approach. *IEEE Transactions on Systems, Man, and Cybernetics: Systems*, 50(11), 4587–4597.
- Lucia, W. and Youssef, A. (2020). Wyner wiretap-like encoding scheme for cyber-physical systems. *IET Cyber-Physical Systems: Theory & Applications*, 5(4), 359–365.
- Lucia, W. and Youssef, A. (2022). A key-agreement scheme for cyber-physical systems. *IEEE Transactions on Systems, Man, and Cybernetics: Systems*, 52(8), 5368–5373.
- Martins, F.N., Sarcinelli-Filho, M., and Carelli, R. (2017). A velocity-based dynamic model and its properties for differential drive mobile robots. *Journal of intelligent & robotic systems*, 85(2), 277–292.
- Maurer, U.M. (1993). Secret key agreement by public discussion from common information. *IEEE transactions on information theory*, 39(3), 733–742.
- Menezes, A.J., Van Oorschot, P.C., and Vanstone, S.A. (2018). *Handbook of applied cryptography*. CRC press.
- Miao, F., Zhu, Q., Pajic, M., and Pappas, G.J. (2016). Coding schemes for securing cyber-physical systems against stealthy data injection attacks. *IEEE Transactions on Control of Network Systems*, 4(1), 106–117.
- Noura, H., Melki, R., Chehab, A., Mansour, M.M., and Martin, S. (2018). Efficient and secure physical encryption scheme for low-power wireless m2m devices. In *International Wireless Communications & Mobile Computing Conference (IWCMC)*, 1267–1272.
- Noura, H.N., Salman, O., Couturier, R., and Chehab, A. (2022). Novel one round message authentication scheme for constrained iot devices. *Journal of Ambient Intelligence and Humanized Computing*, 13(1), 483–499.
- Rawat, D.B., White, T., Parwez, M.S., Bajracharya, C., and Song, M. (2017). Evaluating secrecy outage of physical layer security in large-scale mimo wireless communications for cyber-physical systems. *IEEE Internet of Things Journal*, 4(6), 1987–1993.
- Santilli, M., Franceschelli, M., and Gasparri, A. (2021). Dynamic resilient containment control in multirobot systems. *IEEE Transactions on Robotics*, 38(1), 57–70.
- Shi, X., Shi, S., Wang, M., Kaunisto, J., and Qian, C. (2021). On-device iot certificate revocation checking with small memory and low latency. In *ACM SIGSAC Conference on Computer and Communications Security*, 1118–1134.
- Smith, R.S. (2015). Covert misappropriation of networked control systems: Presenting a feedback structure. *IEEE Control Systems Magazine*, 35(1), 82–92.
- Sutrala, A.K., Obaidat, M.S., Saha, S., Das, A.K., Alazab, M., and Park, Y. (2021). Authenticated key agreement scheme with user anonymity and untraceability for 5g-enabled softwarized industrial cyber-physical systems. *IEEE Transactions on Intelligent Transportation Systems*, 23(3), 2316–2330.
- Tzafestas, S.G. (2013). *Introduction to mobile robot control*. Elsevier.
- Van Assche, G. (2006). *Quantum cryptography and secret-key distillation*. Cambridge University Press.
- Wang, Y., Liu, Q., Mihankhah, E., Lv, C., and Wang, D. (2022). Detection and isolation of sensor attacks for autonomous vehicles: Framework, algorithms, and validation. *IEEE Transactions on Intelligent Transportation Systems*, 23(7), 8247–8259.
- Wang, Z., Yang, S., Xiang, X., Vasilijevic, A., Miskovic, N., and Nad, D. (2021). Cloud-based mission control of usv fleet: Architecture, implementation and experiments. *Control Engineering Practice*. doi:https://doi.org/10.1016/j.conengprac.2020.104657.
- Wyner, A.D. (1975). The wire-tap channel. *Bell system technical journal*, 54(8), 1355–1387.
- Yaacoub, J.P.A., Noura, H.N., Salman, O., and Chehab, A. (2021). Robotics cyber security: Vulnerabilities, attacks, countermeasures, and recommendations. *International Journal of Information Security*, 1–44.
- Zhang, Y., Xiang, Y., and Huang, X. (2017). A cross-layer key establishment model for wireless devices in cyber-physical systems. In *Proceedings of the 3rd ACM Workshop on Cyber-Physical System Security*, 43–53.